Australasian Physical & Engineering Sciences in Medicine (2019) 42:827–838
https://doi.org/10.1007/s13246-019-00767-0

TECHNICAL PAPER

Comparison of muscle synergies extracted from both legs during cycling at different mechanical conditions

Javad Esmaeili[1] · **Ali Maleki**[2]

Received: 8 December 2018 / Accepted: 24 May 2019 / Published online: 3 June 2019

Abstract

Muscle synergies are the building blocks for generating movement by the central nervous system (CNS). According to this hypothesis, CNS decreases the complexity of motor control by combination of a small number of muscle synergies. The aim of this work is to investigate similarity of muscle synergies during cycling across various mechanical conditions. Twenty healthy subjects performed three 6- min cycling tasks at over a range of rotational speed (40, 50, and 60 rpm) and resistant torque (3, 5, and 7 N/m). Surface electromyography (sEMG) signals were recorded during pedaling from eight muscles of the right and left legs. We extracted four synchronous muscle synergies by using the non-negative matrix factorization (NMF) method. Mean and standard deviation of the goodness of the signal reconstruction (R^2) for all subjects was obtained 0.9898 ± 0.0535. We investigated the functional roles of both leg muscles during cycling by synchronous muscle synergy extraction. We compared the muscle synergies extracted from all subjects in all mechanical conditions. The total mean and standard deviation of the similarity of synergy vectors for all subjects in all mechanical conditions was obtained 0.8788 ± 0.0709. We found the high degrees of similarity among the sets of synchronous muscle synergies across mechanical conditions and also across different subjects. Our results demonstrated that different subjects at different mechanical conditions use the same motor control strategies for cycling, despite inter-individual variability of muscle patterns.

Keywords Muscle synergy · Surface electromyography · Nonnegative matrix factorization · Motor control · Cycling

Introduction

Human movements are very complex in a viewpoint of both neural commands and biomechanical process because the central nervous system (CNS) must control and manage various musculoskeletal functions. CNS organizes the involved muscle activations in a movement and coordinates many degrees of freedom with the redundancy of activators of the musculoskeletal system by simplification of motor control in the muscle modules [1]. This redundancy creates flexibility and great smoothing in the motor tasks but complicates the control of these degrees of freedom. CNS coordinates the activation of synergistic muscle groups to simplify many degrees of freedom [2, 3]. Many researchers suggested the low-dimensional muscle activation modules, muscle synergies, to simplify the structure of motor tasks. Neural motor commands recruit muscle synergies to generate the necessary muscle activations to execute motor task. Muscle synergies are as basic blocks that compositions of a small number of them generate a movement in spite of inter-individual variability of muscle signals [4–6].

Muscle synergy is a group of operational elements cooperating together to achieve a demanded motor task [7]. To assess muscle coordination, surface electromyography (sEMG) signals recorded from several muscles involved in a movement can be analyzed into a small number of muscle synergies [8, 9].

Muscle synergies have been already researched for different human movements to define a simplified interpretation for motor control, such as hand reaching movement [10–12], catching movement [13], human walking [14–17], human running [18, 19], and human standing-up [20, 21]. All these

✉ Ali Maleki
amaleki@semnan.ac.ir

Javad Esmaeili
j.esmaeili@semnan.ac.ir

[1] Electrical and Computer Engineering Faculty, Semnan University, Semnan, Iran

[2] Biomedical Engineering Department, Semnan University, Semnan, Iran

works support the being of motor primitives in the modular structure of CNS.

Recently researchers focused also on understanding and extracting muscle synergies during sport practices such as treadmill walking [22–24] and cycling [25–27] to find more verification on the being of simplifying motor control tactics. Cycling can be considered as a constrained and rhythmical exercise with controllable experimental and mechanical conditions comparing to other movements, such as hand reaching or running. Cycling is generally used in biomechanical testing and rehabilitation process.

Recent papers investigated the muscle coordination during pedaling for untrained and trained cyclists or for health and spinal cord injury persons and demonstrated that same muscle synergies are shared and robust through all subjects [28–30]. Recent articles investigated the CNS coordinates and manages neural control mechanisms during pedaling through the pliable combinations of same muscle synergies in response to changes in kinematic parameters such as standing position respect to the seated position in cycling and changes in the kinetics such as velocity, load and torque [3, 30–32].

Previous works have generally focused on synchronous muscle synergy analysis from one leg not both legs [3, 30–32]. In this study, by using synchronous muscle synergies, we investigated the coordination of the muscles of both legs and the functional roles of them during pedaling. We verified that a small number of muscle synergies can cover the variations of EMG patterns from left and right lower limb muscles across various mechanical conditions and different subjects during pedaling.

The aim of the present work was to investigate whether muscle synergies are similar at different mechanical conditions such as resistance torques and rotational speeds during cycling and therefore whether different subjects in various mechanical conditions apply the same motor control tactics for cycling in spite of inter-individual variability of EMG patterns.

Materials and methods

Subjects and experimental protocol

Twenty healthy subjects (ten women and ten men: age, 23–27 years; body mass, 52–75 kg; height, 1.56–1.84 m), with no professional experience, volunteered for the experiments. They were all notified of the inconvenience and possible risk associated with the exercises before signing the consent forms. Subjects practiced on an electronically braked cycle ergometer equipped with standard 0.17 m cranks. Horizontal and vertical positions of the saddle, stem length, and handlebar height were set to match the normal positions of the participants. First, subjects were asked to execute a standardized warm-up inclusive of 5- min of cycling.

The experimental setup consisted of three 6-min cycling tasks at various rotational speeds (40, 50, and 60 rpm). At each rotational speed, first resistant torque was set to 3 N/m until 2 min then were changed to 5 and 7 N/m in every 2-min. In this way, different mechanical conditions were produced to investigate the effect of rotational speed and resistant torque on the muscle synergy extraction during cycling. In this paper the nine cycling tasks were named in the form of Task *i* (rpm, N/m). Figure 1 illustrates these cycling tasks according to experimental setup.

Data recording

Surface electromyography signals were recorded during cycling from eight muscles of the right and left legs: rectus femoris (RF), vastus lateralis (VL), vastus medialis (VM), and biceps femoris (BF) [33, 34].

Eight Bipolar Ag/AgCl electrodes were applied on the chosen muscles. The electrode locations were carefully selected by following the recommendations of the European project; Surface Electromyography for the Non-Invasive Assessment of Muscles (SENIAM) standard [35]. First the skin of special locations for each muscle is shaved and cleaned with alcohol to improve the electrode- skin impedance. Then electrodes were used at these special locations. The electrodes were connected to a pre-amplifier with a gain of 1000 and bandwidth of 20–460 Hz (SX230, Biometrics Ltd., Gwent, UK). The wires of these electrodes were further fixed with adhesive tapes to avoid possible movement-induced artifacts. Each pair of electrodes was regulated as

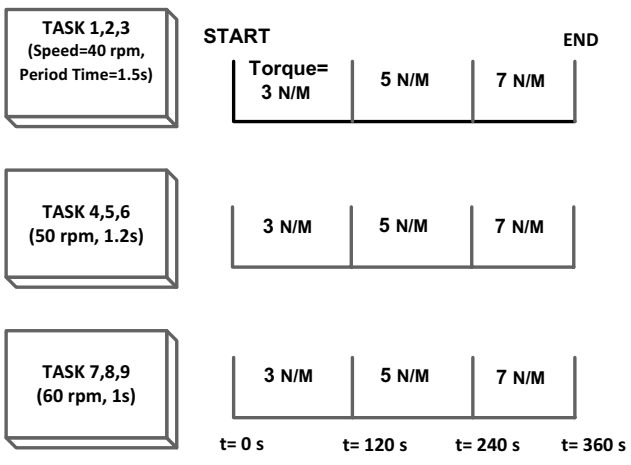

Fig. 1 The experimental protocol consisted of three 6- min cycling tasks at different rotational speeds (40, 50, and 60 rpm). At each rotational speed, first resistance torque was set to 3 N/m until 2-min then were changed to 5 and 7 N/m in every 2-min

much as possible in parallel with the orientation of the muscle fascicles. A common reference electrode (R506, Biometrics Ltd., Gwent, UK) was placed on a bony location, at the distal end of the left ulna.

The hip joint angles and knee joint angles measured by four electrogoniometers in the range of ± 90º with an accuracy of ± 2º (SG150, Biometrics Ltd., Gwent, UK). sEMG signals were gathered with a portable data acquisition system equipped with four digital channels and eight analog channels, with the range of sampling frequency per analog channel 1 up 20,000 Hz and with an accuracy better than ± 0.5% full scale (DataLOG-MWX8, Biometrics Ltd., Gwent, UK).

A pedaling cycle was defined as the complete revolution of the crank starting from highest position of the pedal with crank arm angle at 0° (TDC; Top Dead Center), passing through lowest position of the pedal with crank arm angle at 180° (BDC; Bottom Dead Center) and back to TDC in a 360° [36]. The pedaling cycle can be divided into two phases [37]:

Power phase: From TDC to BDC. The power phase occurs as the hip and knee extends, pressing downward on the pedal. First a combination of the gluteus maximus (GM) and quadriceps (rectus femoris (RF), vastus lateralis (VL), vastus medialis (VM), vastus intermedius (VI)) are activated to extend the knee and then hamstrings (such as biceps femoris (BF)) are activated to extend the hip.

Recovery phase: From BDC to TDC. During the recovery phase the hip flexor muscles, the iliopsoas and the rectus femoris (RF) are activated and then hamstrings (such as biceps femoris (BF)) are activated to knee flexion. The rectus femoris (RF) contracts during the last stage of the recovery phase to flex the hip in preparation for the next pedal stroke.

sEMG signal preprocessing

sEMG signals were high-pass filtered (fifth order Butterworth filter, cutoff 10 Hz) to remove artifacts and reduce noise, and then they were full-wave rectified and low-pass filtered (fourth order Butterworth filter, cutoff 3 Hz) in order to earn the linear envelopes [33, 38]. Each muscle waveform was normalized to its maximum amplitude from all of the sequential pedaling cycles. Each envelope was averaged across five sequential pedaling cycles in order to obtain an indicator activation pattern for each muscle in each condition.

Synchronous muscle synergy analysis

In the synchronous muscle synergies analysis, muscle activation signals ($m_i(t), 1 \le i \le n$) are represented by the linear combination of non-negative muscle synergies ($w_{ij}, 1 \le j \le N$) in which the number of muscle synergies (N) is less than the number of muscle activation signals (n) [39]:

$$m_i(t) = \sum_{j=1}^{N} c_j(t) w_{ij}, i = 1, \ldots, n \quad (1)$$

where $c_j(t)$ is a non-negative scalar coefficient of the jth muscle synergy at time t, and w_{ij} is a time-independent weight for ith muscle. In fact, muscle synergies are fixed activation patterns among several muscles and synergy coefficients are signals that the CNS produces them to control the muscle synergies (i.e. neural commands). Matrix form of synchronous muscle synergy equation is shown as [40]:

$$\mathbf{M}_{n\times N} = \mathbf{W}_{n\times k}\mathbf{C}_{k\times N} \quad (2)$$

where $\mathbf{M}$ is muscle activation data matrix, $\mathbf{W}$ is muscle synergy matrix, $\mathbf{C}$ is synergy coefficient matrix, and k denotes the number of muscle synergies ($k \le \min(n, N)$).

Such analysis is called synchronous synergy model because in this model, muscle synergies can occur simultaneously. Figure 2 illustrates two sets of synchronous muscle synergies with different scaling coefficients. Four muscle patterns are produced by combination of two sets of synchronous muscle synergies and their scaling coefficients. We used synchronous muscle synergy model in this work.

Several dimensionality reduction algorithms have been used to extract synchronous muscle synergies underlying various human movements [42]: Principal component analysis (PCA), Independent component analysis (ICA) and Nonnegative matrix factorization (NMF). We selected NMF algorithm among these techniques, because NMF algorithm forces a

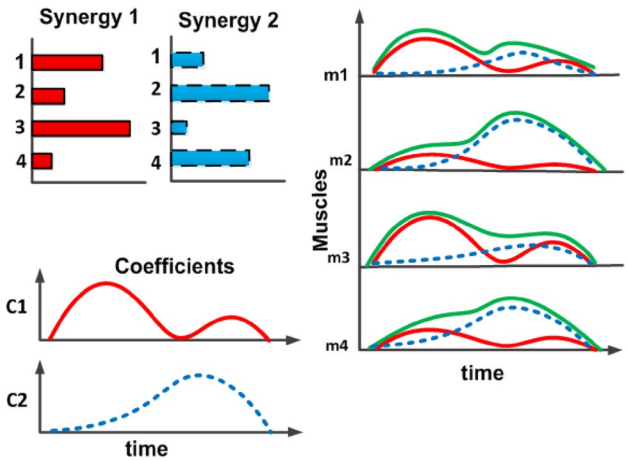

Fig. 2 Concept of synchronous muscle synergy model: An example of four muscle patterns (*right*) construction based on two set of synchronous muscle synergies (*left*) with scaling coefficients (C_1,C_2). Different muscle patterns are produced by using two set of synergies and changing values of two scaling coefficients

non-negativity limitation to the extracted muscle synergies [42]. This limitation reflects well the attributes of muscle activation patterns, as muscles are always activated non-negativity. Moreover, PCA and ICA techniques impose specific assumptions among the extracted muscle synergies (orthogonality for PCA and statistical independence for ICA), which force limitations between the corresponding muscle synergies. NMF algorithm does not force such limitations and thus seems more acceptable for studying about muscle synergy extraction [47].

The non-negative matrix factorization (NMF) algorithm decomposes a non-negative matrix **M** into two non-negative factors; **W** and **C**, that is:

$$\mathbf{M} = \mathbf{WC} + \mathbf{E} \tag{3}$$

where **E** is the reconstruction error or residual. NMF algorithm is optimized by minimizing the frobenius norm as [41]:

$$\min_{\mathbf{W},\mathbf{C}} \frac{1}{2}\mathbf{M} - \mathbf{WC}_{\mathrm{F}}^{2}, \text{subject to }, \mathbf{W}, \mathbf{C} \geq 0 \tag{4}$$

where $\|*\|_F^2$ represents the squared frobenius norm of a matrix. NMF algorithm is the most common muscle synergy extraction algorithm. NMF algorithm was used to calculate synchronous muscle synergies [42, 43]. Synergy vectors (**W**) and synergy coefficients (**C**) are selected at the NMF algorithm, to minimize the total reconstruction error. NMF algorithm minimizes reconstruction error by updating coefficients using synergies, and updating next muscle synergies by using modified coefficients. It iterates until the reconstruction error is minimized [44].

Most of the papers used R^2 [17, 45, 46] or VAF [15, 47, 48] criteria to evaluate the results of muscle synergy analysis. R^2 parameter represents the fraction of total variation accounted for by the muscle synergy reconstruction. The goodness of muscle synergy approximation is described as R^2 [5]:

$$R^2 = 1 - \frac{SSE}{SST} = 1 - \frac{\left\|\mathbf{M} - \hat{\mathbf{M}}\right\|_{\mathrm{F}}^{2}}{\left\|\mathbf{M} - \bar{\mathbf{M}}\right\|_{\mathrm{F}}^{2}} \tag{5}$$

where **M** is a non-negative matrix ($\mathbf{M} \in \mathcal{R}_{+}^{N\times n}$) of muscle activation signals, $\hat{\mathbf{M}} = \mathbf{WH}$ is the approximated **M** matrix, and *SSE* is the sum of the squared residuals, and *SST* represents the sum of the squared residual from the mean activation signals (sum of squared residuals from the mean of the **M** matrix ($\bar{\mathbf{M}}$)). R^2 as a statistical Parameter represents proximity of the approximated data to the fitted regression line. Also other goodness of the signal reconstruction in muscle synergy analysis is computed by *VAF* [5]:

$$VAF = 1 - \frac{SSE}{SST} = 1 - \frac{\left\|\mathbf{M} - \hat{\mathbf{M}}\right\|_{\mathrm{F}}^{2}}{\|\mathbf{M}\|_{\mathrm{F}}^{2}} \tag{6}$$

where *SST* is the total sum of squares that is computed on uncentered data (sum of squares of residuals from zero). We used customary criteria, R^2 and *VAF* to measure the accuracy of the signal reconstruction in muscle synergy analysis.

Choice of the number of muscle synergies

The number of extracted muscle synergies (N) is an important parameter of the synchronous muscle synergy model [49]. The appropriate number of muscle synergies was described as the conciliation between model parsimony and reconstruction accuracy, observing the relationship between the amount of data variation in the goodness of the signal reconstruction (R^2) and the number of muscle synergies.

Mean of R^2 for all subjects at different mechanical conditions is used to determine how many muscle synergies are sufficient to explain the cycling task. We used R^2 versus N plot to select the desired number of muscle synergies. The proper number of muscle synergies was selected as the number that in which the slope of the R^2 curve had a noticeable variation, indicating that additional muscle synergies only enveloped slight residual amounts of variation attributable to noise. Generally this slope change happened in the amount of more than 0.9 for the curve of R^2 [50]. The computed number of synchronous muscle synergies by this process could reconstruct the slight differences of each dataset of the cycling task.

Synchronous muscle synergy comparison

The angle cosine between two synchronous muscle synergy vectors was evaluated as a criterion of their similarity. Similarity value was defined as the maximum of the normalized scalar products between two sets of synchronous muscle synergies [19].

We compared the synchronous muscle synergies extracted from each subject in different mechanical conditions and also from the same mechanical condition in different subjects. To compare two sets of synchronous muscle synergies, extracted from different subjects or different mechanical conditions, we computed the similarities between their best matching pairs were computed. First the pair with the maximum similarity values was chosen, and then the synchronous muscle synergies of this choice pair from their sets were removed. Finally, the similarities between remaining synchronous muscle synergies were computed and were chosen the next best matching pair [24, 51].

Results

For all subjects (ten women and ten men) and all cycling tasks, according to the experimental protocol, EMG waveforms were recorded from eight muscles of the left and right

legs; rectus femoris (LRF and RRF), vastus lateralis (LVL and RVL), vastus medialis (LVM and RVM), and biceps femoris (LBF and RBF). Then EMG waveforms were high-pass filtered and were full-wave rectified and low-pass filtered in order to earn the linear envelopes. Each EMG activity pattern was normalized to its maximum amplitude from all of the sequential pedaling cycles. Figure 3 shows example of averaged EMG activity patterns from five sequential pedaling cycles in order to obtain a representative EMG activity patterns for each muscle.

We extracted synchronous muscle synergies with a number of muscle synergies ranging from two to seven by using the muscle patterns for all subjects and all mechanical conditions by NMF method. The number of muscle synergies was chosen to consider for better analysis as conciliation between model parsimony and reconstruction accuracy. As seen in Fig. 4 the curve of the R^2 as a function of the number of synchronous muscle synergies has a change in the slope at four. The being of a knee point in the curve of the R^2 demonstrated that muscle synergy sets with more number of muscle synergies at the knee point described only a small additional fraction of the data variation (R^2). Hence, for all subjects at nine cycling tasks, four synchronous muscle synergies were chosen as the proper number of muscle synergies.

We decomposed muscle patterns as the combination of four synchronous muscle synergies, each one with a specific scaling coefficient. Figure 5 shows four sets of synchronous muscle synergies extracted from eight muscle patterns during cycling by NMF method for functional interpretation. It represents the basic features of the muscle synergies

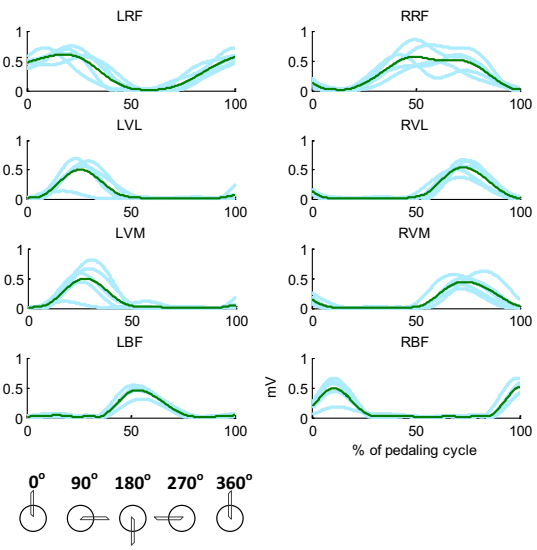

Fig. 3 Example of averaged EMG activity patterns and crank angle for a pedaling cycle. Mean EMG activity patterns across five sequential pedaling cycles for Subject 1 in Task 4 (50 rpm, 3 N/m) from four muscles of the left (L) and right (R) legs. Abbreviations for muscles are mentioned in "Materials and methods"

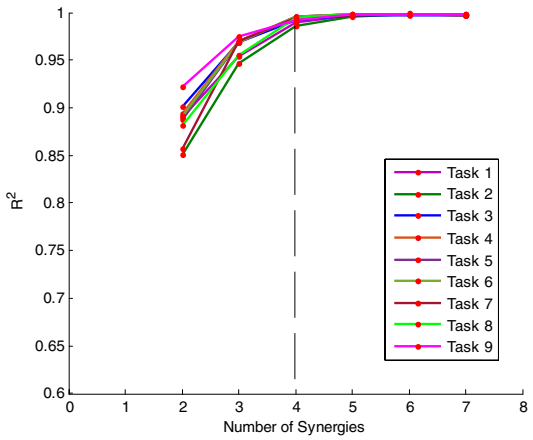

Fig. 4 Selection of the number of muscle synergies extracted from muscle patterns during cycling: For each number of muscle synergy ranging from two to seven, synchronous muscle synergy extraction are performed on each mechanical condition (Task 1 to Task 9) for all subjects then mean and standard deviation of (R^2) are computed and shown. In all subjects and conditions, four muscle synergies were selected as the appropriate number of muscle synergies

(synergy vectors and scaling coefficients) extracted from all subjects for nine cycling tasks.

By analyzing of the synergy vectors and the scaling coefficients, some properties were distinguished for each synchronous muscle synergy. Four synchronous muscle synergies include different features of the muscle patterns in the pedaling cycle: Synergy 1 indicates knee extension of the left leg. Synergy 2 indicates knee flexion/hip extension of the left leg and knee extension/hip flexion of the right leg. Synergy 3 indicates knee extension of the right leg. Synergy 4 indicates knee flexion/hip extension of the right leg and knee extension/flexion of the left leg. Table 1 represents function, involved leg muscles and range of pedaling cycle for each synchronous muscle synergy.

For each subject and each cycling task, four synchronous muscle synergies are scaled in amplitude according to specific coefficients and then summed together for producing all muscle patterns (see Materials and methods). The activation EMG waveforms for all leg muscles were exactly reconstructed by the combinations of the muscle synergies. The example of the EMG pattern reconstruction for subject 1 in Task 4 (50 rpm, 3 N/m) by the combinations of the four synchronous muscle synergies is shown in Fig. 6. The performance analysis criteria for reconstruction of all muscle patterns such as VAF(%) and R^2 were obtained 99.9311% and 0.9993 respectively.

Table 2 shows mean and standard deviation of the VAF(%) and R^2 values for reconstructed EMG patterns of all subjects in each mechanical condition (A), and for each subject in all mechanical conditions (B) by four sets of synchronous muscle synergies combinations.

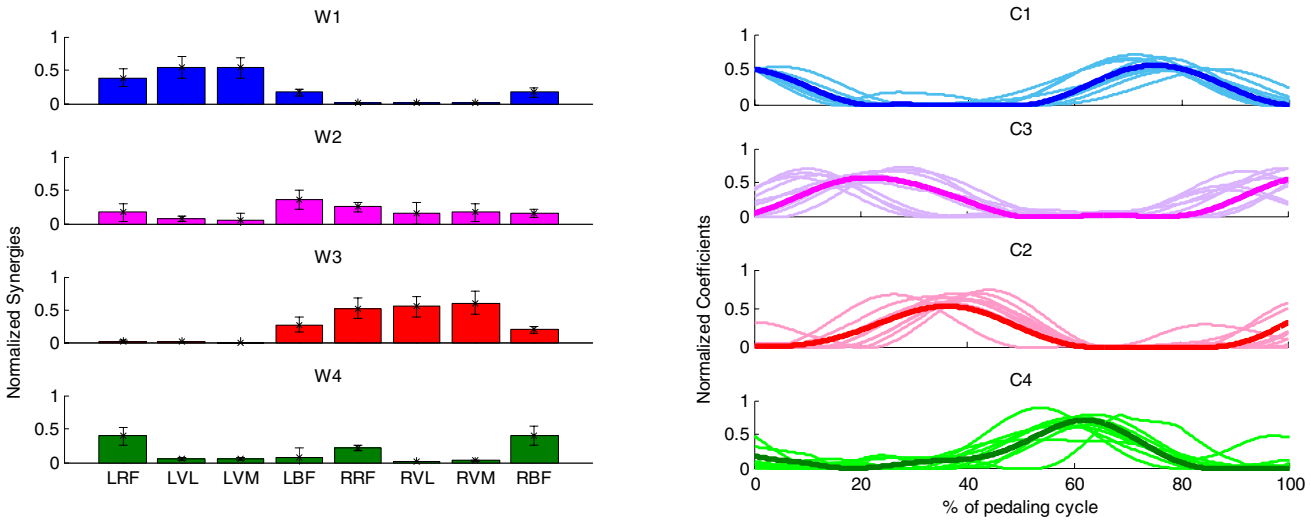

Fig. 5 Four sets of synchronous muscle synergies are extracted from eight muscle patterns during cycling. The basic features of the muscle synergies (synergy vectors and scaling coefficients) extracted from all subjects for nine cycling tasks. Abbreviations for muscles are mentioned in "Materials and methods"

Table 1 Four synchronous muscle synergies and their functions, involved muscles and range of pedaling cycle

Synergies	Function	Muscles	Rang of pedaling cycle
Synergy 1	Knee extension of left leg	Quadriceps group of left leg (VL, VM, and RF)	Power phase
Synergy 2	Knee flexion/hip extension of left leg and knee extension/hip flexion of right leg	Hamstrings group of left leg (BF) and RF of right leg	Middle part of the power phase and the beginning of the recovery phase
Synergy 3	Knee extension of right leg	Quadriceps group of right leg (VL, VM, and RF)	Recovery phase
Synergy 4	Knee flexion/hip extension of right leg and knee extension/flexion of left leg	Hamstrings group of right leg (BF) and RF of left leg	Middle part of the recovery phase and the beginning of the power phase

RF rectus femoris, *VL* vastus lateralis, *VM* vastus medialis, *BF* biceps femoris

Similarity criterion was used to survey the comparison of synchronous muscle synergies. Similarity between two sets of synchronous muscle synergies is defined as the maximum of their normalized scalar product.

We compared the muscle synergies extracted by NMF method from the same mechanical condition in different subjects. Figure 7 shows comparison of synchronous muscle synergies between two subjects from each mechanical condition. In Fig. 7, the similarity of "Synergies" and "Coefficients" between four pairs of synchronous muscle synergies extracted from two subjects (for example subject 12 and subject 13) for all mechanical conditions (Task 1 to Task 9) are shown. The total mean and standard deviation of the similarity of "Synergies" for all tasks is 0.8788 ± 0.0709 and total mean and standard deviation of the similarity of "Coefficients" for all tasks is 0.8413 ± 0.0679. This comparison demonstrates that there are high degrees of similarity between two sets of synchronous muscle synergies extracted from the same mechanical condition in different subjects.

We also compared the muscle synergies extracted by NMF method from each subject in different mechanical conditions. Figure 8 shows comparison of synchronous muscle synergies extracted from one subject in different mechanical conditions. We compared synchronous muscle synergies extracted from Task 1 (40 rpm, 3 N/m) with other tasks and synchronous muscle synergies extracted from Task 2 (40 rpm, 5 N/m) with other tasks, etcetera. Then mean and standard deviation of all similarity values was computed. In Fig. 8, mean and standard deviation of the similarity values of "Synergies" and "Coefficients" between four pairs of synchronous muscle synergies extracted from one subject (for example, subject 1) for all mechanical conditions (Task 1 to Task 9) are shown. The total mean and standard deviation of the similarity of "Synergies" for all mechanical conditions

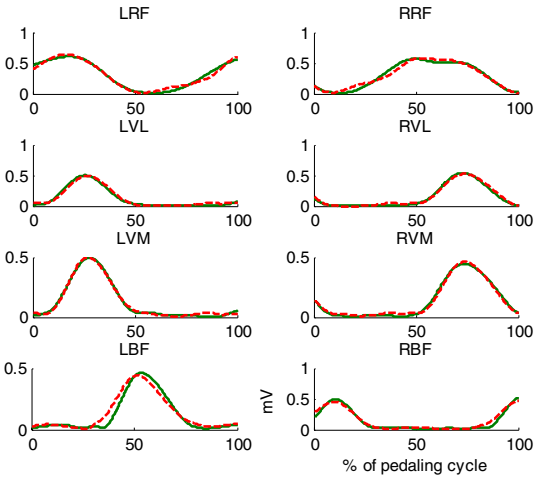

Fig. 6 Example of reconstructed muscle patterns by synchronous muscle synergy combination. Muscle patterns are reconstructed by four independently scaled synchronous muscle synergies extracted from EMG activity patterns of Subject 1 in Task 4 (50 rpm, 3 N/m). Abbreviations for muscles are mentioned in "Materials and methods"

is 0.8128 ± 0.0305 and total mean and standard deviation of the similarity of "Coefficients" for all mechanical conditions is 0.7962 ± 0.0292. This comparison demonstrates that there are significant similarities between two sets of the synchronous muscle synergies extracted from one subject in different mechanical conditions.

We also compared the synchronous muscle synergies extracted from all subjects in each mechanical condition separately. Table 3-A shows mean and standard deviation of the similarity values of "Synergies" between four pairs of synchronous muscle synergies extracted from all subjects for each mechanical condition and Table 3-B shows mean and standard deviation of the similarity values of "Coefficients" of them. The total mean and standard deviation of the similarity of "Synergies" for all subjects in all mechanical conditions is 0.8788 ± 0.0709 and total mean and standard deviation of the similarity of "Coefficients" for all subjects in all mechanical conditions is 0.8413 ± 0.0679. This comparison also demonstrates the high degree of similarities between synchronous muscle synergies across all subjects in all mechanical conditions.

Discussion

Four muscle synergies well describe sEMG signals

In this study, we used a previously-developed procedure to verify how the CNS produces motor coordination [3, 31]. Four synchronous muscle synergies were extracted during cycling over a range of rotational speed (40, 50, and 60 rpm) and resistant torque (3, 5, and 7 N/m) from 20 healthy subjects. The total mean and standard deviation of R^2 value for reconstructed muscle patterns of all subjects in all mechanical conditions was calculated 0.9898 ± 0.0535.

In this paper, the results showed that the combinations of a few synchronous muscle synergies, with proper scaling in amplitude, explain many characteristics of the sEMG patterns recorded from eight muscles of the right and left legs during cycling across different mechanical conditions. We used NMF method [42, 43] to find the basic features of the synchronous muscle synergies (synergy vectors and scaling coefficients) extracted from all subjects for nine cycling tasks.

In previous works [3, 30, 31] sEMG signals were recorded from 8-11 lower limb muscles during cycling. They extracted three [3] or four [30, 31] synchronous muscle synergies by using the NMF method. In previous research, three synchronous muscle synergies were extracted to explain function of lower limb muscles during pedaling. They proposed to investigation the existence of a fourth muscle synergy in future studies [3]. The results of the present study are in agreement with the recent works [30, 31] that reported that four muscle synergies account for the majority of variability in the sEMG signals of lower limb muscles during pedaling. Fourth muscle synergy is used to explain function of hip and knee flexor muscles during the middle part of the recovery phase and during the beginning of the power phase of the pedaling cycle. Moreover, trained cyclists participated in the previous study [3]. Different number of muscle synergies in the previous study [3] may be due to reflect the ability of them to merge different muscle synergies. Trained cyclists may be able to achieve muscle coordination during pedaling by fewer synergies [31]. This query can be tested on future studies by focus on the differences of the extracted muscle synergies between trained and untrained subjects.

Functional interpretation of the extracted muscle synergies

By analyzing of the synergy vectors and the scaling coefficients from four synchronous muscle synergy extracted by the NMF method (Fig. 5), the following properties are distinguished for each synchronous muscle synergy during pedaling:

Synergy 1 represents knee extension of the left leg. This synergy consists of knee extensor activity from the three muscles of the quadriceps group of the left leg (vastus lateralis, vastus medialis, and rectus femoris). This synergy is active during the power phase of the pedaling cycle.

Synergy 2 represents knee flexion/hip extension of the left leg and knee extension/hip flexion of the right leg. This synergy consists of activity in the hamstrings group of the left leg (biceps femoris) and consists of the activity in the rectus femoris of the right leg. This synergy is active during

Table 2 Mean and standard deviation of the VAF (%), and R^2 value for reconstructed muscle patterns of all subjects in each mechanical condition (A), and for each subject in all mechanical conditions (B), by four synchronous muscle synergies combinations

(A)

Speed (rpm)	Torque (N/m)	VAF (%)	R^2
40	3	99.1088 ± 0.576	0.9845 ± 0.0024
	5	98.6923 ± 1.0731	0.9793 ± 0.0255
	7	98.8411 ± 1.0788	0.9843 ± 0.0132
50	3	99.1916 ± 0.6297	0.9842 ± 0.0081
	5	99.3904 ± 0.4007	0.9928 ± 0.0040
	7	99.4118 ± 0.5160	0.9926 ± 0.0072
60	3	99.1130 ± 0.6061	0.9862 ± 0.0093
	5	99.5280 ± 0.3121	0.9929 ± 0.0056
	7	99.5547 ± 0.4010	0.9931 ± 0.0012

(B)

Subject	VAF (%)	R^2
S1	99.3345 ± 0.4092	0.9876 ± 0.0088
S2	99.5259 ± 0.3519	0.9911 ± 0.0106
S3	99.3488 ± 0.0404	0.9920 ± 0.0043
S4	99.4689 ± 0.0121	0.9940 ± 5.1765e−04
S5	98.4585 ± 0.5307	0.9820 ± 0.0015
S6	99.5018 ± 0.1476	0.9935 ± 0.9935
S7	99.3315 ± 0.3831	0.9902 ± 0.0016
S8	98.8606 ± 0.0626	0.9767 ± 0.0079
S9	99.6063 ± 0.0847	0.9929 ± 0.0033
S10	99.5197 ± 0.2188	0.9939 ± 0.0031
S11	99.0503 ± 0.2783	0.9859 ± 0.0038
S12	99.4265 ± 0.5459	0.9924 ± 0.0079
S13	99.4950 ± 0.1975	0.9929 ± 0.0029
S14	99.6260 ± 0.1255	0.9938 ± 0.0035
S15	98.9765 ± 0.3089	0.9809 ± 0.0043
S16	98.5155 ± 0.4107	0.9817 ± 0.0083
S17	99.6473 ± 0.0353	0.9945 ± 9.6521e−04
S18	99.4927 ± 0.1977	0.9935 ± 0.0012
S19	99.3320 ± 0.0625	0.9919 ± 0.0014
S20	99.4593 ± 0.1618	0.9938 ± 0.0015

the middle part of the power phase and during the beginning of the recovery phase.

Synergy 3, similar to synergy 1, represents knee extension of the right leg. This synergy consists of knee extensor activity from the three muscles of the quadriceps group of the right leg. This synergy is active during the recovery phase of the pedaling cycle.

Synergy 4, similar to synergy 2, represents knee flexion/hip extension of the right leg and knee extension/flexion of the left leg. This synergy consists of activity in the hamstrings group of the right leg and consists of the activity in the rectus femoris of the left leg. This synergy is active during the middle part of the recovery phase and during the beginning of the power phase.

Previous studies investigated coordination of the muscles of one leg [3, 30–32]. In this research, the extraction of synchronous muscle synergies has been done in both legs. The results indicated the co-operation and coordination of the muscles of both legs. When one of the legs is in the first phase of pedaling, the other is in the second phase, and the activity of the RF muscle in each leg is almost synchronous with the BF muscle of the other leg. The greater part of the activity of the VL and VM muscles of each leg coincides with the activity of the RF muscle and part of its activity with the RF muscle of the other leg.

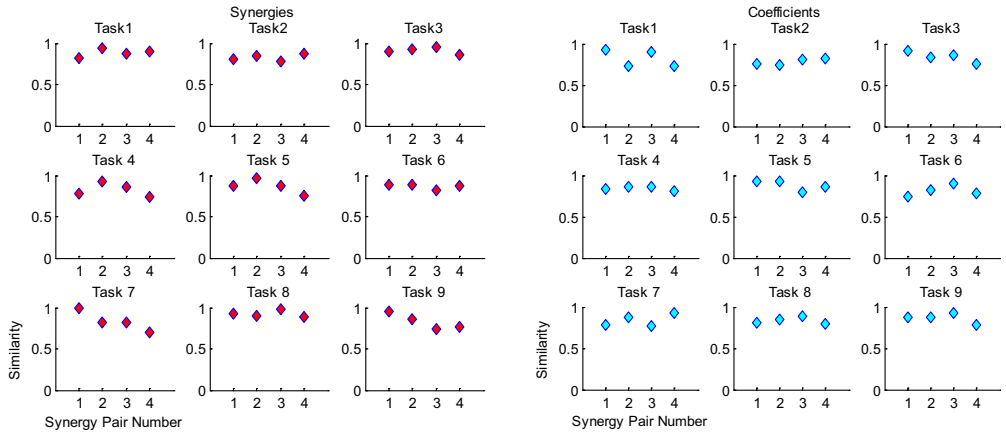

Fig. 7 Comparison of muscle synergies between two subjects from each mechanical condition. Each one of the left nine plots shows the similarity of "Synergies" between each pairs of four muscle synergies extracted from two subjects (for example subject 12 and subject 13) for all mechanical conditions. Each one of the right nine plots shows the similarity of "Coefficients" between them

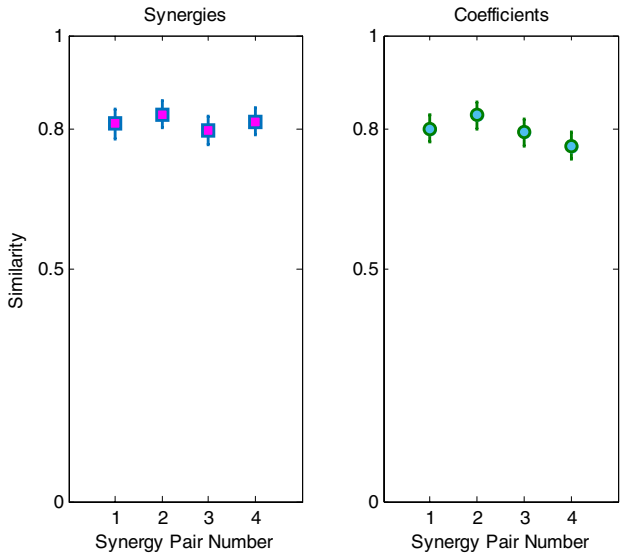

Fig. 8 Comparison of muscle synergies extracted from one subject in different mechanical conditions. Mean and standard deviation of the similarity values of "Synergies" and "Coefficients" between each pairs of four muscle synergies extracted from one subject (for example subject 1) for all mechanical conditions are shown

Comparison of muscle synergies

The main purpose of this work is to investigate the effect of rotational speed and resistant torque on the muscle synergy extraction during cycling. Therefore, we compared the sets of synchronous muscle synergies extracted from different subjects and different mechanical conditions by the NMF method.

As performed in previous works [31, 32], we also evaluated the similarity of each of these four sets of synchronous muscle synergies across subjects. According to the high similarity values found for "Synergies" (0.9003, 0.8955, 0.8779 and 0.8415 for synergies 1–4, respectively) and "Coefficients" (0.8584, 0.8577, 0.8173 and 0.8312 for synergies 1–4, respectively), we can conclude that the four similar functional synchronous muscle synergies are used by each subject (Table 3). Despite differences in torque-velocity scenarios during pedaling [3, 28] and difference in posture (standing or seated position) [30] between our study and other works, similarity values for muscle synergy vectors and synergy activation coefficients are obtained like them more than 0.8. Thus we can hypothesize that same locomotor strategies during pedaling motion are used by each subject.

By comparing the sets of synchronous muscle synergies extracted from individual tasks, results showed significant similarities among synergies. These similarities demonstrate the being of sufficient amount of shared structure in the control of movement in different mechanical conditions. We also compared the sets of synchronous muscle synergies extracted from the same mechanical condition in different subjects. Results showed the high degree of similarities among subjects, demonstrating the being of a common basic structure of the patterns displayed by the muscle synergies for all individuals.

Although four set of muscle synergies were similar across all mechanical conditions, the individual synergy vectors and coefficients were in some cases more variable. Hence, similarity values for some cases of synergy vectors and coefficients were obtained lower than 0.8 (Table 3). These differences may reflect subject-specific motion patterns and represent the musculoskeletal redundancy in attainment the stability during pedaling task. Although differences in anatomy may proceed to differences in muscle synergies, it is probable that training and motor skill for cyclists also impressed subject-specific motion patterns [14]. In addition,

Table 3 Comparison of the muscle synergies across all subjects in each mechanical condition. Mean and standard deviation of the similarity values of "Synergies" (A) and similarity values of "Coefficients" (B), among sets of synchronous muscle synergies extracted from all subjects for each mechanical condition

(A)

Speed (rpm)	Torque (N/m)	Synergy 1	Synergy 2	Synergy 3	Synergy 4
40	3	0.8925 ± 0.0695	0.8525 ± 0.1490	0.9719 ± 0.0119	0.7306 ± 0.1699
	5	0.9134 ± 0.0317	0.9350 ± 0.0446	0.9008 ± 0.0498	0.7885 ± 0.1891
	7	0.8866 ± 0.0150	0.8252 ± 0.0646	0.9427 ± 0.0260	0.9103 ± 0.0759
50	3	0.8915 ± 0.0134	0.9207 ± 0.0709	0.7393 ± 0.1340	0.8420 ± 0.0547
	5	0.8352 ± 0.0439	0.8443 ± 0.0755	0.9774 ± 0.0585	0.9297 ± 0.0139
	7	0.9526 ± 0.0382	0.9625 ± 0.0276	0.7593 ± 0.1224	0.7157 ± 0.1149
60	3	0.9103 ± 0.0766	0.8464 ± 0.0680	0.9062 ± 0.0751	0.9520 ± 0.0258
	5	0.8490 ± 0.0795	0.9698 ± 0.0655	0.8812 ± 0.1025	0.9331 ± 0.0841
	7	0.9715 ± 0.0187	0.9033 ± 0.0163	0.8229 ± 0.1506	0.7720 ± 0.1254

(B)

Speed (rpm)	Torque (N/m)	Synergy 1	Synergy 2	Synergy 3	Synergy 4
40	3	0.8159 ± 0.0814	0.8262 ± 0.0831	0.8453 ± 0.0076	0.9106 ± 0.0337
	5	0.9468 ± 0.0244	0.7071 ± 0.1585	0.7652 ± 0.1054	0.8193 ± 0.1162
	7	0.7526 ± 0.1929	0.8217 ± 0.0550	0.8606 ± 0.0531	0.7680 ± 0.1794
50	3	0.7441 ± 0.1350	0.9183 ± 0.0417	0.8496 ± 0.0279	0.8366 ± 0.0311
	5	0.7782 ± 0.0197	0.8930 ± 0.0286	0.8319 ± 0.0934	0.8382 ± 0.0529
	7	0.9316 ± 0.0251	0.7523 ± 0.1757	0.7653 ± 0.1130	0.8849 ± 0.0166
60	3	0.9864 ± 0.0616	0.9578 ± 0.0354	0.7822 ± 0.0569	0.9324 ± 0.0206
	5	0.8559 ± 0.0173	0.9829 ± 0.0380	0.8131 ± 0.0469	0.7402 ± 0.1263
	7	0.9174 ± 0.0052	0.8607 ± 0.0168	0.8440 ± 0.0012	0.7506 ± 0.1654

these differences may be due to appear some lag times for the torque and posture effects [3]. Timing is an important parameter in motor control for human movements. Hence, we suggest the time-varying muscle synergy analysis introduced by d'Avella and et al. [10, 13, 51] for future studies. In the time-varying muscle synergy analysis, sEMG waveforms are described as linear combinations of muscle synergies by scaling in amplitudes and shifting in times.

In this study, practices of cycling and synchronous muscle synergy analysis were performed only on the healthy subjects, so it would be useful to guide additional analysis on non-healthy subjects. If synchronous muscle synergies are extracted from individuals with cerebral palsy or disorder or spinal cord injury, such information could be helpful in rehabilitation or aided devices to recovery and improvement limb function [21, 29].

Conclusions

The main benefit of this paper is support the statement that the CNS uses a modular organization of muscles to reduce the complication of motor control. Our results show that these modules can be repeated across various cycling tasks. The modular organization of motor control can be applied to control neuro-rehabilitative tools such as neuro-prosthesis based on functional electrical stimulation (FES), to restore neuromuscular function and rehabilitate in paresis patients [52, 53]. In the robotic fields this repeatability decreases the computational space and can improve the pliability of robotic motion [54–56].

Compliance with ethical standards

Conflict of interest The authors declare that there are no conflicts of interest with this paper.

Ethical approval All procedures performed in studies involving human participants were in accordance with the ethical standards of the 1964 Helsinki declaration and its later amendments or comparable ethical standards.

Informed consent Informed consent was obtained from all individual participants included in the study.

References

1. Bernstein NA (1967) The co-ordination and regulation of movements. Pergamon Press, London
2. Latash ML, Gorniak S, Zatsiorsky VM (2008) Hierarchies of synergies in human movements. Kinesiology 40:29–38
3. Hug F, Turpin NA, Couturier A, Dorel S (2011) Consistency of muscle synergies during pedaling across different mechanical constraints. J Neurophysiol 106(1):91–103
4. Ting LH, Chvatal SA (2010) Decomposing muscle activity in motor tasks. In: Danion F, Latash ML (eds) Motor control theories, experiments and applications. Oxford University Press, New York, pp 102–138
5. De Rugy A, Loeb GE, Carroll TJ (2013) Are muscle synergies useful for neural control? Front Comput Neurosci 7:19
6. d'Avella A, Giese M, Ivanenko YP, Schack T, Flash T (2015) Modularity in motor control: from muscle synergies to cognitive action representation. Front Comput Neurosci 9:126
7. Latash ML (2010) Stages in learning motor synergies: a view based on the equilibrium-point hypothesis. Hum Mov Sci 29(5):642–654
8. Oliveira AS, Gizzi L, Farina D, Kersting UG (2014) Motor modules of human locomotion: influence of EMG averaging, concatenation, and number of step cycles. Front Hum Neurosci 8:335
9. Costa-García A, Itkonen M, Yamasaki H, Shibata-Alnajjar F, Shimoda S (2018) A novel approach to the segmentation of sEMG data based on the activation and deactivation of muscle synergies during movement. IEEE Robot Autom Lett 3(3):1972–1977
10. d'Avella A, Lacquaniti F (2013) Control of reaching movements by muscle synergy combinations. Front Comput Neurosci 7:42
11. Coscia M, Cheung VC, Tropea P, Koenig A, Monaco V, Bennis C, Micera S, Bonato P (2014) The effect of arm weight support on upper limb muscle synergies during reaching movements. J Neuroeng Rehabil 11(1):22
12. Scano A, Chiavenna A, Malosio M, Molinari Tosatti L, Molteni F (2017) Muscle synergies-based characterization and clustering of poststroke patients in reaching movements. Front Bioeng Biotechnol 5:62
13. D'Andola M, Cesqui B, Fernandez L, D'Avella A (2013) Spatiotemporal characteristics of muscle patterns for ball catching. Front Comput Neurosci 7:107
14. Chvatal SA, Ting LH (2013) Common muscle synergies for balance and walking. Front Comput Neurosci 7:48
15. Kim Y, Bulea TC, Damiano DL (2016) Novel methods to enhance precision and reliability in muscle synergy identification during walking. Front Hum Neurosci 10:455
16. Rimini D, Agostini V, Knaflitz M (2017) Evaluation of muscle synergies stability in human locomotion: a comparison between normal and fast walking speed. In: IEEE international instrumentation and measurement technology conference (I2MTC), Turin, Italy, IEEE. https://doi.org/10.1109/I2MTC.2017.7969722
17. Jacobs DA, Koller JR, Steele KM, Ferris DP (2018) Motor modules during adaptation to walking in a powered ankle exoskeleton. J Neuroeng Rehabil 15(1):2
18. Matsunaga N, Imai A, Kaneoka K (2017) Comparison of muscle synergies before and after 10 minutes of running. J Phys Ther Sci 29(7):1242–1246
19. Nishida K, Hagio S, Kibushi B, Moritani T, Kouzaki M (2017) Comparison of muscle synergies for running between different foot strike patterns. PLoS ONE 12(2):e0171535
20. An Q, Yamakawa H, Yamashita A, Asama H (2017) Different temporal structure of muscle synergy between sit-to-walk and sit-to-stand motions in human standing leg. Converging clinical and engineering research on neurorehabilitation II. Biosys Biorobot 15:933–937. https://doi.org/10.1007/978-3-319-46669-9_151
21. Yang N, An Q, Yamakawa H, Tamura Y, Yamashita A, Asama H (2017) Clarification of muscle synergy structure during standing-up motion of healthy young, elderly and post-stroke patients. In: IEEE international conference on rehabilitation robotics (ICORR), London, UK, IEEE, pp 19–24. https://doi.org/10.1109/ICORR.2017.8009215
22. Oliveira AS, Gizzi L, Ketabi S, Farina D, Kersting UG (2016) Modular control of treadmill vs overground running. PLoS ONE 11(4):e0153307
23. Saito A, Tomita A, Ando R, Watanabe K, Akima H (2018) Similarity of muscle synergies extracted from the lower limb including the deep muscles between level and uphill treadmill walking. Gait Posture 59:134–139
24. Kibushi B, Hagio S, Moritani T, Kouzaki M (2018) Speed-dependent modulation of muscle activity based on muscle synergies during treadmill walking. Front Hum Neurosci 12:4
25. De Marchis C, Castronovo AM, Bibbo D, Schmid M, Conforto S (2012) Muscle synergies are consistent when pedaling under different biomechanical demands. In: 34th Annual international conference of the IEEE Engineering in Medicine and Biology Society (EMBS), San Diego, California, USA, pp 3308–3311. https://doi.org/10.1109/EMBC.2012.6346672
26. Saito A, Watanabe K, Akima H (2015) Coordination among thigh muscles including the vastus intermedius and adductor magnus at different cycling intensities. Hum Mov Sci 40:14–23
27. Torricelli D, Tobaruela DN, De Marchis C, Barroso F, Pons JL (2016) Is modular control of cycling affected by learning? Preliminary results using muscle biofeedback. In: Converging clinical and engineering research on neurorehabilitation II;Biosys Biorobot 15:919–923
28. Hug F, Turpin NA, Guével A, Dorel S (2010) Is interindividual variability of EMG patterns in trained cyclists related to different muscle synergies? J Appl Physiol 108(6):1727–1736
29. Barroso FO, Torricelli D, Bravo-Esteban E, Taylor J, Gómez-Soriano J, Santos C, Moreno JC, Pons JL (2015) Muscle synergies in cycling after incomplete spinal cord injury: correlation with clinical measures of motor function and spasticity. Front Hum Neurosci 9:706
30. Turpin NA, Costes A, Moretto P, Watier B (2017) Can muscle coordination explain the advantage of using the standing position during intense cycling? J Sci Med Sport 20(6):611–616
31. De Marchis C, Schmid M, Bibbo D, Bernabucci I, Conforto S (2013) Inter-individual variability of forces and modular muscle coordination in cycling: a study on untrained subjects. Hum Mov Sci 32(6):1480–1494
32. De Marchis C, Severini G, Castronovo AM, Schmid M, Conforto S (2015) Intermuscular coherence contributions in synergistic muscles during pedaling. Exp Brain Res 233(6):1907–1919
33. Hug F, Dorel S (2009) Electromyographic analysis of pedaling: a review. J Electromyogr Kinesiol 19(2):182–198
34. Momeni K, Faghri PD, Evans M (2014) Lower-extremity joint kinematics and muscle activations during semi-reclined cycling at different workloads in healthy individuals. J Neuroeng Rehabil 11(1):146
35. Tang L, Li F, Cao S, Zhang X, Wu D, Chen X (2015) Muscle synergy analysis in children with cerebral palsy. J Neural Eng 12(4):046017
36. Blake OM, Champoux Y, Wakeling JM (2012) Muscle coordination patterns for efficient cycling. Med Sci Sports Exerc 44(5):926–938
37. So RC, Ng JKF, Ng GY (2005) Muscle recruitment pattern in cycling: a review. Phys Ther Sport 6(2):89–96
38. Hug F (2011) Can muscle coordination be precisely studied by surface electromyography? J Electromyogr Kinesiol 21(1):1–12
39. McKay JL, Ting LH (2007) Functional muscle synergies constrain force production during postural tasks. J Biomech 41(2):299–306

40. Wojtara T, Alnajjar F, Shimoda S, Kimura H (2014) Muscle synergy stability and human balance maintenance. J Neuroeng Rehabil 11(1):129
41. Li Y, Ngom A (2013) The non-negative matrix factorization toolbox for biological data mining. Source Code Biol Med 8(1):10
42. Tresch MC, Cheung VC, d'Avella A (2006) Matrix factorization algorithms for the identification of muscle synergies: evaluation on simulated and experimental data sets. J Neurophysiol 95(4):2199–2212
43. Cheung VC, Piron L, Agostini M, Silvoni S, Turolla A, Bizzi E (2009) Stability of muscle synergies for voluntary actions after cortical stroke in humans. Proc Natl Acad Sci USA 106(46):19563–19568
44. Berry MW, Browne M, Langville AN, Pauca VP, Plemmons RJ (2007) Algorithms and applications for approximate nonnegative matrix factorization. Comput Stat Data An 52(1):155–173
45. Choi C, Kim J (2011) Synergy matrices to estimate fluid wrist movements by surface electromyography. Med Eng Phys 33(8):916–923
46. Gentner R, Edmunds T, Pai DK, d'Avella A (2013) Robustness of muscle synergies during visuomotor adaptation. Front Comput Neurosci 7:120
47. Delis I, Berret B, Pozzo T, Panzeri S (2013) A methodology for assessing the effect of correlations among muscle synergy activations on task-discriminating information. Front Comput Neurosci 7:54
48. Chiovetto E, Huber ME, Sternad D, Giese MA (2018) Low-dimensional organization of angular momentum during walking on a narrow beam. Sci Rep 8(1):95
49. Steele KM, Tresch MC, Perreault EJ (2013) The number and choice of muscles impact the results of muscle synergy analyses. Front Comput Neurosci 7:105
50. d'Avella A, Portone A, Lacquaniti F (2011) Superposition and modulation of muscle synergies for reaching in response to a change in target location. J Neurophysiol 106(6):2796–2812
51. d'Avella A, Portone A, Fernandez L, Lacquaniti F (2006) Control of fast-reaching movements by muscle synergy combinations. J Neurosci 26(30):7791–7810
52. Quandt F, Hummel FC (2014) The influence of functional electrical stimulation on hand motor recovery in stroke patients: a review. Exp Transl Stroke Med 6(1):9
53. Toledo-Peral CL, Gutiérrez-Martínez J, Mercado-Gutiérrez JA, Martín-Vignon-Whaley AI, Vera-Hernández A, Leija-Salas L (2018) sEMG signal acquisition strategy towards Hand FES Control. J Healthc Eng. https://doi.org/10.1155/2018/2350834
54. Alessandro C, Delis I, Nori F, Panzeri S, Berret B (2013) Muscle synergies in neuroscience and robotics: from input-space to task-space perspectives. Front Comput Neurosci 7:43
55. Ison M, Artemiadis P (2015) Proportional myoelectric control of robots: muscle synergy development drives performance enhancement, retainment, and generalization. IEEE Trans Robot 31(2):259–268
56. Taborri J, Agostini V, Artemiadis PK, Ghislieri M, Jacobs DA, Roh J, Rossi S (2018) Feasibility of muscle synergy outcomes in clinics, robotics, and sports: a systematic review. Appl Bionics Biomech. https://doi.org/10.1155/2018/3934698